Journal of Marine Science and Technology
https://doi.org/10.1007/s00773-019-00642-3

ORIGINAL ARTICLE

Application of optimal control theory based on the evolution strategy (CMA-ES) to automatic berthing

Atsuo Maki[1] · Naoki Sakamoto[2] · Youhei Akimoto[3] · Hiroyuki Nishikawa[1] · Naoya Umeda[1]

Received: 29 June 2018 / Accepted: 9 April 2019

Abstract
To realize autonomous ships in the near future, possibility of automatic berthing has been investigated. Automatic berthing is not an easy task because of some complexities that are included in the problem, such as the nonlinearity of the low-speed maneuvering model, danger of collision with berth, etc. In this research, as a first step, the authors solved the off-line automatic berthing problem. Here, the optimal control problem was modeled as minimum-time problem, and the collision risk with the berth was taken into account. The authors attempted to apply the covariance matrix adaption evolution strategy (CMA-ES), which is considered state-of-the-art in evolutionary computation approaches for optimization of real-valued variables. In the problem dealt with here, a propeller and a rudder were used only as control inputs; so, the degree of difficulty was significantly high. Nevertheless, optimal control method based on the CMA-ES successfully gave us the offline results for typical situations considered. It is noteworthy that preparation of a feasible initial control input was not required in the calculation process, which made the proposed procedure robust. The calculation method proposed here is offline, but the results could be applied as an initial guess in an online (real-time) control problem.

Keywords Autonomous vessel · Automatic berthing · Optimal control theory · Evolution strategy · CMA-ES

1 Introduction

To realize autonomous vessels in the future, a fundamental research on automatic berthing has been carried out. Autonomous operation is now proceeding in other vehicle areas such as cars, and in our field, many research projects are in progress [1, 2]. One of the purposes of autonomous operation is to save labor and provide safe transportation. On the road to the final goal, there are many technical issues to be solved. One of them is automatic berthing. Automatic berthing is not an easy task due to some complexities. For instance, a ship has huge inertia; so, it cannot be stopped easily like a car. Furthermore, in the low-speed region, control inputs such as the rudder force are relatively small compared with the high-speed maneuvering condition. Moreover, in low-speed regions, the hydrodynamic modeling has many difficulties and complexities.

Since the 1970s, researchers in Japan have boldly pursued a solution to this difficult problem. From 1983 to 1988, extensive research projects on the automatic control of ships were carried out, and among those projects, automatic berthing systems were studied as an important topic. It is noteworthy that with the use of the automatic berthing system constructed in this project, full-scale experiments were conducted using the training vessel "Shioji-Maru" [3, 4]. As pointed out by Hasegawa [5], automation projects for berthing in a port area were unique in the world at that time, which meant that the technical level of Japanese researchers and engineers was considered highest.

On the topic of automation, the first study in the public domain was conducted by Kose et al. [6] in 1986. In his approach, he first obtained the maneuvering plan to be guided, and then the desired trajectory was followed by feedback and feed-forward control. However, this berthing

✉ Atsuo Maki
maki@naoe.eng.osaka-u.ac.jp

[1] Department of Naval Architecture and Ocean Engineering, Graduate School of Engineering, Osaka University, 2-1 Yamadaoka, Suita, Osaka 565-0971, Japan

[2] Graduate School of Medicine, Science and Technology, Shinshu University, 4-17-1 Wakasato, Nagano, Nagano 380-8553, Japan

[3] Faculty of Engineering, Information and Systems, University of Tsukuba, 1-1-1 Tennodai, Tsukuba, Ibaraki 305-8573, Japan

Published online: 02 May 2019

control is based upon support by a tugboat. In 1987, Koyama et al. modeled the berthing problem as an optimal regulator problem, and in his novel research, it is noteworthy that he took account of the collision risk to the berth in the objective function as the penalty function [7]. On the other hand, in 1990, Yamato et al. showed the automatic berthing results using a neural network [8]. Following his success, Hasegawa et al. [9] also has contributed to the automatic berthing research with the neural network. Furthermore, Yamato et al. [10] applied an expert system and then showed successful berthing results for more complex situations, in which another vessel coexists in the same port area.

Another important approach is a use of nonlinear optimal control theory, which also has long history. The first report in the public domain was carried out by Shouji et al. [11]. In this research, they applied the sequential conjugate gradient restoration algorithm (SCGRA) [12] method, which is based upon a variational method. It showed optimal berthing results in the solution of a minimum-time problem. These approaches have great advantages because they are based on mathematical theory. For instance, constraints can be taken into account without difficulties, if necessary. After their first report, Shouji et al. conducted further researches on automatic berthing for a vessel with side thrusters and controllable-pitch propellers (CPP) [13, 14]. Following their success, Okazaki et al. [15] also utilized the SCGRA method and solved the minimum-time stop maneuver problem. A recent hot topic in the research field of optimal control is the progress of a real-time optimal control technique known as model predictive control. The one state-of-the-art technique in real-time optimal control is the continuous/generalized minimum residual (C/GMRES) method proposed by Ohtsuka [16]. The application results of this method for cable-laying maneuvers of a vessel were reported [17]. Although the methodology is not the same as C/GMRES, Mizuno et al. recently (2015) reported the results of model predictive control in optimal berthing control [18].

In the final stage of berthing control, very difficult and precise control is required to avoid collision against the berth or port equipment. However, in the most of the past studies (except for Koyama [7]), the results in which the collision risks had been considered could not be found. The main reason for this is that if the collision risks are taken into account, the constraint functions and the objective function could make the problem to be solved too complex. So far, although the SCGRA method or the method based upon mathematical programming has been utilized, which are based on a gradient method, these methods often fail to solve the complex problem.

For robust optimal control, the choice of the calculation method is important, and the quality of the solution may strongly depend on the used optimization method. For instance, the authors investigated the rudder control of a ship in following and quartering seas by using an optimal control theory. Then, two solution methods, i.e., the SCGRA method and a mathematical programming method called sequential quadratic programming (SQP) method, were applied [19, 20]. Ultimately, the latter algorithm overwhelmed the former one from the perspective of robustness and convergence. However, since the SQP method is a gradient method, the quality of the final result (i.e., the local optimal solution) completely depends on the initial guess of the optimal input. Therefore, within the framework of the gradient-based search method, only the local optimal solution that exists around a given initial guess can be searched. Furthermore, to avoid infeasible solutions, a high-quality prior solution should be prepared in the beginning. However, to find these solution candidates, time-consuming effort is usually required and sometimes fails.

In this research, the authors attempted to solve the berthing problem in light of the optimal control theory. As a first step, automatic berthing control was modeled as a minimum-time problem. Since this was offline (not real-time) control, the results are not directly applicable to online (real-time) control. However, advances in the online optimal berthing control method could not be achieved without a method that robustly and certainly generates an optimal input offline. To achieve this goal, the authors attempted to apply the covariance matrix adaption evolution strategy (CMA-ES) [21, 22] which is considered state-of-the-art in evolutionary computation, and the optimal berthing problem was subsequently solved. The application of the evolution strategy to the optimal control problem is not new. For instance, Yokoyama and Suzuki [23] utilized the unimodal normal distribution crossover (UNDX-m) [24] method, which is known as one of the real-coded genetic algorithms (GAs) to the optimal path generation problem of spacecraft. They concluded that the numerical method using the GA simultaneously and effectively achieved a global and feasible search [23]. In this research, following this methodology, the numerical method using the CMA-ES is proposed and applied to the ship berthing problem. In the problem dealt with here, the main thruster and rudder are used only as control inputs. Of course, the maneuvering model is highly nonlinear, and in the performance index, the collision risk to the berth is taken into account; so, the degree of difficulty is significantly high. This paper shows how the numerical optimization method using the CMA-ES works well for this highly nonlinear problem.

2 Maneuvering simulation model

The authors here show the coordinate systems in Fig. 1, and the origin of the ship's fixed coordinate ones is the midship. The equation of motion is based on the maneuvering modeling group (MMG) modeling method [25] as follows:

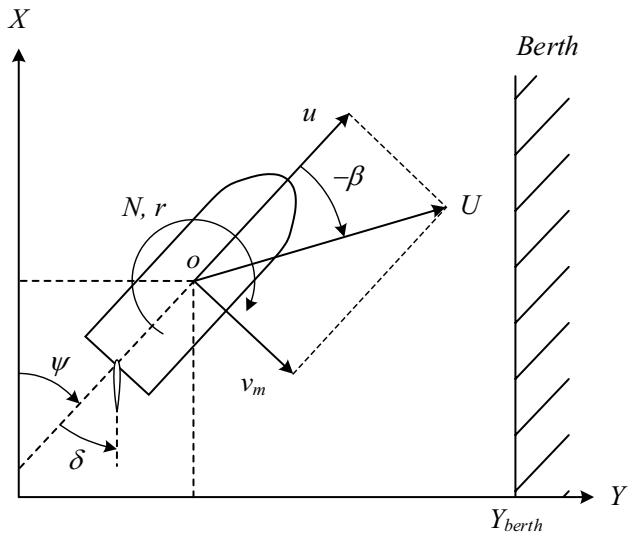

Fig. 1 Coordinate systems

$$\begin{cases} (m+m_x)\dot{u} - (m+m_y)v_{\mathrm{m}}\, r \;=\; X \\ (m+m_y)\dot{v}_{\mathrm{m}} + (m+m_x)u\, r = Y. \\ (I_{zz}+J_{zz})\dot{r} + x_{\mathrm{G}}m(\dot{v}_{\mathrm{m}} + ur) = N_{\mathrm{m}} \end{cases} \tag{1}$$

In Eq. (1), the right-hand side can be represented as

$$\begin{cases} X \;=\; X_{\mathrm{H}} + X_{\mathrm{P}} + X_{\mathrm{R}} \\ Y = Y_{\mathrm{H}} + Y_{\mathrm{P}} + Y_{\mathrm{R}} \\ N_{\mathrm{m}} = N_{\mathrm{H}} + N_{\mathrm{R}} + N_{\mathrm{P}} \end{cases}, \tag{2}$$

and the lateral velocity at midship v_{m} is calculated as

$$v_{\mathrm{m}} = v - x_{\mathrm{G}}r. \tag{3}$$

In these equations, u, v, and r represent the surge velocity, sway velocity at the center of gravity, and yaw angular velocity, respectively. The overdot denotes differentiation with respect to time t. In addition, m, ship's mass; m_x, x directional-added mass; m_y, y directional-added mass; I_{zz}, yaw moment of inertia; J_{zz}, yaw-added moment of inertia; x_G, x directional position of the center of gravity. On the right-hand side, X, Y, and N represent the surge force, yaw force, and sway moment, and the subscripts H, P, and R denote the hull, propeller, and rudder components. The non-dimensionalization in this paper is as follows:

$$\begin{cases} \text{Velocity}' = \text{Velocity}/U \\ \text{Force}' = \text{Force}/\dfrac{1}{2}\rho L d_{\mathrm{s}} U^2 \\ \text{Moment}' = \text{Moment}/\dfrac{1}{2}\rho L^2 d_{\mathrm{s}} U^2 \end{cases}. \tag{4}$$

The prime symbol denotes a nondimensional value. Here, water density; L, ship's length; d_{s}, ship's draft; and U is the resultant speed:

$$U = \sqrt{u^2 + v_{\mathrm{m}}^2}. \tag{5}$$

The force acting on the hull is estimated by Yoshimura's method, in which linear hydrodynamic forces and crossflow drag forces are taken into account [26]. He confirmed that this estimation mode is applicable for very wide range of maneuvering motions:

$$\begin{cases} X_{\mathrm{H}} / \dfrac{1}{2}\rho L \mathrm{d} U^2 = \left[X'_{0\,(F)} + \left(X'_{0\,(A)} - X'_{0\,(F)}\right)(|\beta|/\pi)\right]uU \\ \quad + X'_{\mathrm{vr}}\, v_{\mathrm{m}} r \\ Y_{\mathrm{H}} / \dfrac{1}{2}\rho L \mathrm{d} U^2 = Y'_{\mathrm{v}} v_{\mathrm{m}}|u| + Y'_{\mathrm{r}}\, ru \\ - \dfrac{C_{\mathrm{D}}}{L}\displaystyle\int_{-L/2}^{L/2} \left|v_{\mathrm{m}} + C_{\mathrm{rY}} rx\right|\left(v_{\mathrm{m}} + C_{\mathrm{rY}} rx\right)\mathrm{d}x \\ N_{\mathrm{H}} / \dfrac{1}{2}\rho L^2 \mathrm{d} U^2 = N'_{\mathrm{v}} v_{\mathrm{m}} u + N'_{\mathrm{r}} r|u| \\ - \dfrac{C_{\mathrm{D}}}{L^2}\displaystyle\int_{-L/2}^{L/2} \left|v_{\mathrm{m}} + C_{\mathrm{rN}} rx\right|\left(v_{\mathrm{m}} + C_{\mathrm{rN}} rx\right)x\mathrm{d}x \end{cases}. \tag{6}$$

In this equation, $X_{0\,(F)}$ is the ahead resistance coefficient, whereas $X_{0\,(A)}$ is the astern resistance coefficient. Here, the value of C_{D} can be estimated as Y'_{H} at $\beta = 90°$, whereas C_{rY} and C_{rN} are correction factors for the lateral force and yaw moments. Now, the drifting angle β is defined as

$$\beta = \tan^{-1}\left(-v_{\mathrm{m}}/u\right). \tag{7}$$

The subject ship used here is a geometric scale model (length: 3 m) of super tanker MV Esso Osaka, e.g., [27–29], and its main characteristics are shown in Table 1. In addition, the hydrodynamic coefficients used here are listed in Table 2, e.g., [27–29].

Propeller forces are estimated by the model based on the forward and backward propeller rotations and the forward and backward ship moving speeds. In the case of $n > 0$,

$$\begin{cases} X_{\mathrm{P}} = \rho D_{\mathrm{P}}^4 n^2 \left(1 - t_{\mathrm{P}}\right) K_{\mathrm{T}} \\ Y_{\mathrm{P}} = 0 \\ N_{\mathrm{P}} = 0 \end{cases}, \tag{8}$$

where t_{P} is the thrust reduction coefficient, and coefficient K_{T} is represented as a quadratic polynomial with respect to J:

$$K_{\mathrm{T}} = a_1 + a_2 J + a_3 J^2. \tag{9}$$

Here, J is the advance coefficient, which is represented as

Table 1 Main characteristics in model scale

Item	Value
Ship length: L_{pp}	3.00 m
Ship breadth: B	0.49 m
Ship draft: d	0.20 m
Block coefficients: C_b	0.83

Table 2 Maneuvering coefficients, e.g., [27–29]

Hull		Propeller		Rudder	
$X'_{0(F)}$	–0.02139	D_P	0.08400 m	A_R	0.01063 m^2
$X'_{0(A)}$	–0.03189	P/D	0.7151	λ	1.539
X'_{vr}	0.4535	w_{P0}	0.6140	ε	1.420
Y'_{v}	–0.3728	τ	0.8710	a_H	0.3930
Y'_{r}	0.1160	C'_P	–0.3590	k	0.2880
N'_{v}	–0.1458	a_1	0.3278	t_R	0.1900
N'_{r}	–0.04849	a_2	–0.3223	γ_P	0.3506
C_D	0.9665	a_3	–0.1560	γ_N	0.4406
C_{rY}	2.127	t_P	0.2200		
C_{rN}	0.8097				

$$J = \frac{u(1-w_P)}{nD_P}, \tag{10}$$

where D_P is the propeller diameter and n is the propeller revolution number. In the above equation, the wake coefficient at propeller position w_P is estimated as

$$1 - w_P = 1 - w_{P0} + \tau\left|v'_m + x'_P r'\right| + C'_P\left(v'_m + x'_P r'\right)^2,, \tag{11}$$

where w_{P0} is the wake coefficient in the straight-ahead moving condition, and τ and C'_P are experimentally determined coefficients. In the case of $n<0$, empirical expressions obtained from the past towing tank test results are utilized:

$$X_P = \rho n^2 D_P^4 \begin{Bmatrix} C_1 + C_2 J_S & (J_S \geq C_{10}) \\ C_3 & (J_S < C_{10}) \end{Bmatrix}. \tag{12}$$

Here, $J_S = u/nD_P$.

$$Y_P = \frac{1}{2}\rho L\, d(nD_P)^2 \begin{Bmatrix} A_1 + A_2 J_S & (J_{syn} \leq J_S \leq J_{syn0}) \\ A_3 + A_4 J_S & (J_S < J_{syn}) \\ A_5 & (J_{syn0} < J_S) \end{Bmatrix},, \tag{13}$$

$$N_P = \frac{1}{2}\rho L^2 d(nD_P)^2 \begin{Bmatrix} B_1 + B_2 J_S & (J_{syn} \leq J_S \leq J_{syn0}) \\ B_3 + B_4 J_S & (J_S < J_{syn}) \\ B_5 & (J_{syn0} < J_S) \end{Bmatrix}. \tag{14}$$

The coefficients used here [A_i ($i=1$–3), B_i ($i=1$–5),C_i ($i=1$–5)] are listed in Table 3 [29].

The rudder forces are also estimated by the model based on the forward and backward propeller rotations and the forward and backward ship moving speeds. These expressions still have room for argument, but as a first step in the research, the following expressions are utilized. For $n>0$,

$$\begin{cases} X_R &= -(1-t_R)F_N \sin\delta \\ Y_R &= -(1+a_H)F_N \cos\delta\,. \\ N_R &= -(x_R + a_H x_H)F_N \cos\delta \end{cases} \tag{15}$$

In the case of $n>0$ and $u>0$,

$$\begin{cases} F_N = \frac{1}{2}\rho A_R f_\alpha U_R^2 \sin\alpha_R \\ U_R = \sqrt{u_R^2 + v_R^2} \end{cases}. \tag{16}$$

In the case of $n>0$ and $u<0$,

$$\begin{cases} F_N = -\frac{1}{2}\rho A_R U_R^2 \sin\alpha_R \\ U_R = \sqrt{u_R^2 + v_R^2} \end{cases}. \tag{17}$$

In the equations above, each term can be calculated as shown below. Here, the rudder lift gradient coefficient f is estimated using Fujii's formula [30]:

$$f_\alpha = \frac{6.13}{2.25 + \Lambda}. \tag{18}$$

Here, Λ is an aspect ratio of the rudder:

$$u_R = u_P\left[\varepsilon + k_x\left(\sqrt{1 + 8K_T/\pi J^2} - 1\right)\right]. \tag{19}$$

In the above equation, ε and k_x are ratios of the wake fraction at propeller and rudder positions, and the experimental

Table 3 Propeller coefficients [29]

A_1	–7.90E–05	B_1	3.50E–05	C_3	–0.2668	J_{syn}	–0.35
A_2	7.99E–03	B_2	–3.17E–03	C_6	–0.257	J_{syn0}	–0.06
A_3	–4.93E–03	B_3	1.96E–03	C_7	0.51	J_{st}	–0.6
A_4	–5.87E–03	B_4	2.33E–03	C_{10}	–0.233		
A_5	–5.58E–04	B_5	2.25E–04				

constant for calculating u_R, respectively. Furthermore, in Eq. (17), v_R is calculated as

$$v_R = \gamma'(v + l_R r), \tag{20}$$

where γ is the flow-straightening coefficient, and l_R is the effective longitudinal coordinate of the rudder position. In Eq. (17), α_R is the effective inflow angle of the rudder:

$$\alpha_R = \delta + \tan^{-1}(v_R / u_R). \tag{21}$$

Here, δ is the rudder angle. In this research, the external wind force is not taken into account. This effect should be considered in online (real-time) control in our future research.

In the case of $n < 0$, the authors assume that the propeller does not generate the forces [31].

3 Optimal control problem

In this paper, optimal berthing is modeled as a minimum-time problem. In the beginning, the state equation can be represented in vector form:

$$\dot{\mathbf{x}} = \mathbf{f}(\mathbf{x}, \mathbf{u}). \tag{22}$$

The state and control vectors are defined as

$$\begin{cases} \mathbf{x} \equiv (x,\ u, y, v,\ \psi, r)^T \in \mathbf{R}^6 \\ \mathbf{u} \equiv (\delta\,(t),\ n\,(t))^T \in \mathbf{R}^2 \end{cases}, \tag{23}$$

where x is the x-directional position, y is the y-directional position, and ψ is the yaw angle. The problem to be solved is a two-point boundary problem in which the initial and final states are fixed. Now, let t_f be the final time, and the next non-dimensional time τ is introduced:

$$\tau = t / t_f. \tag{24}$$

Introduction of the non-dimensional time in Eq. (22) becomes

$$\dot{\mathbf{x}} = t_f \mathbf{f}(\mathbf{x}, \mathbf{u}). \tag{25}$$

Then, the time span becomes $\tau \in [0,\ 1]$, which is convenient for programming. Hereafter, the overdot denotes differentiation with respect to the non-dimensional time τ. In the berthing problem, the initial and final conditions are explicitly given as

$$\begin{cases} \mathbf{x}\,(0) = \mathbf{x}_0 \\ \mathbf{x}\,(1) = \mathbf{x}_1 \end{cases}, \tag{26}$$

where $\mathbf{x}_0$ and $\mathbf{x}_1$ are the vectors of the initial and final conditions, respectively. The rudder and propeller revolution numbers are bounded; so, the constraints on the control input were imposed on these values as

$$\begin{cases} \delta^2(\tau) - \delta_{\max}^2 \le 0 \\ n^2(\tau) - n_{\max}^2 \le 0 \end{cases}. \tag{27}$$

Since this optimal control problem is solved as minimum-time problem, the fundamental form of the objective function is the final time t_f:

$$J_0 \equiv t_f. \tag{28}$$

In the current framework of the CMA-ES, the equality constraints cannot be taken into account, so the authors extend the objective function using the weight w_1:

$$J_1 \equiv t_f + w_1 \left| \mathbf{x}\,(1) - \mathbf{x}_1 \right|. \tag{29}$$

It is desirable that the berthing be achieved in as short a time as possible, but the most important thing is to avoid a collision with the port or berth. With regard to this point, as mentioned in the introduction, Koyama indeed solved the automatic berthing problem in the framework of an optimal regulator problem and took account of the collision risk in the objective function [7]. Following his approach, the authors defined the function C, which has a value only if the vertex of the rectangle surrounding the ship is inside the berth. Equation (30) represents the calculation formula. Here, let P_i $(i = 1\text{–}4)$ be the four vertices of the rectangle surrounding the ship:

$$C = \sum_{i=1}^{4} \int_{P_i \in C_{\text{berth}}} |Y_i - Y_{\text{berth}}| \mathrm{d}t. \tag{30}$$

In this equation, C_{berth} denotes the area inside the berth, Y_i denotes each Y ordinate of P_i, and Y_{berth} denotes each Y ordinate of the berth. In Koyama's research [7], because of the limitations of the optimal regulator problem, the distance between the berth and ship was taken into account in the quadratic form. In this research, the solver in the optimal control problem is not a gradient-based method; so, the expression in absolute value does not become a problem. Finally, the extended objective function is represented as:

$$J_1 \equiv t_f + w_1 \left| \mathbf{x}\,(1) - \mathbf{x}_1 \right| + w_2 C, \tag{31}$$

where w_2 is the weight for collision risk. In this paper, w_1 and w_2 are 1.0×10^5 and 5.0×10^6, respectively. The unknown variables to be optimized are the final time t_f and the control inputs (i.e., the rudder angle δ and propeller revolution number n). For numerical computation, the control inputs are discretized in $m - 1$ segments, and in each segment, the control input is assumed to be changed linearly. As a result, the unknown variable vector $\mathbf{X}$ to be optimized is represented as

$$\mathbf{X} \equiv \left(t_f,\ \delta_1, \ldots, \delta_m,\ n_1, \ldots, n_m\right)^{\mathrm{T}} \in \mathbf{R}^{2m+1}. \tag{32}$$

In this paper, m is 21.

Summarizing the above, original problem to be solved is:

$$\begin{aligned}
\text{minimize} \ : \quad & J_1 = t_\mathrm{f} \\
\text{subject to} \ : \quad & \dot{\mathbf{x}} = t_\mathrm{f}\mathbf{f}(\mathbf{x}, \mathbf{u}) \\
& \mathbf{x}(0) = \mathbf{x}_0 \\
& \delta^2(\tau) - \delta^2_{\max} \le 0, \ \ n^2(\tau) - n^2_{\max} \le 0 \\
& \left|\mathbf{x}(1) - \mathbf{x}_1\right| \le \varepsilon \\
& C = 0.
\end{aligned} \tag{33}$$

Here, by introducing the weights w_1 and w_2, the problem to be solved becomes:

$$\begin{aligned}
\text{minimize} \ : \quad & J_1 = t_\mathrm{f} + w_1\left|\mathbf{x}(1) - \mathbf{x}_1\right| + w_2 C \\
\text{subject to} \ : \quad & \dot{\mathbf{x}} = t_\mathrm{f}\mathbf{f}(\mathbf{x}, \mathbf{u}) \\
& \mathbf{x}(0) = \mathbf{x}_0 \\
& \delta^2(\tau) - \delta^2_{\max} \le 0, \ \ n^2(\tau) - n^2_{\max} \le 0.
\end{aligned} \tag{34)}$$

Here, the weight parameters in the objective function (i.e., penalty coefficient) are set as large values to strictly satisfy the terminal condition and avoid the collision. As the first two lines of the above constraints are treated by the penalization in the objective, an optimization algorithm only needs to treat the box constraints defined for each rudder and propeller revolution numbers. Another possible approach would be to formulate the terminal condition as inequality constraints by allowing small error in each coordinate, and apply a sophisticated inequality constraint handling method for CMA-ES, such as augmented Lagrangian constraint handling method [32], which makes it free from tuning of the penalty coefficients as the algorithm automatically does. We leave it for a future work and focus on the fixed penalty method as described above in the following of the paper.

4 CMA-ES

As stated above, the authors applied the CMA-ES [21, 22], which is considered state-of-the-art in evolutionary computation approached in continuous domain. This method is applicable for a problem having a rugged search landscape, such as discontinuities, ill-conditioning, and variable dependencies. In contrast to quasi Newton methods [e.g., the sequential quadratic programming (SQP) method], the CMA-ES does not require a gradient calculation. This makes the method robust and feasible, even for a non-continuous problem. With each iteration, new search points are generated stochastically using a multivariate normal distribution, and the distribution parameters such as the mean vector and the covariance matrix are updated with successful candidate solutions and their objective value ranking. One of the great advantages in the application of the CMA-ES is that time-consuming parameter tuning is not required. The parameter choice is not a user task, except for population size. In this research, the latest CMA-ES algorithm adopted to box constraints (inequality constraints) [34, 35] was utilized. This algorithm uses the automatic restart [36] with increasing population size, i.e., the number of candidate solutions generated in an iteration.

Figure 2 illustrates the procedure of the CMA-ES. The multivariate normal distribution is identified by the equi-density ellipsoid, where the distribution center is determined by the mean vector and the distribution shape and spread are determined by the covariance matrix. Note that the direction and length of each axis of the equi-density ellipsoid are given by the unit eigenvector and the square root of the eigenvalue of the covariance matrix, respectively. The CMA-ES samples multiple candidate solutions and evaluate them on the objective function. The covariance matrix and the mean vector are updated, so that the likelihood of sampling promising candidate solutions is increased. This update is known to decrease the expected objective value in the steepest descent direction in the parameter space [37]. The distribution spread is further updated to accelerate the search and to make the search more robust. The sampling–evaluation–update step is repeated until some stopping conditions such as too small distribution spread or maximum number of function evaluations are met.

Algorithm: CMA-ES

1. Set $\mathbf{m}^{(0)}$, $\sigma^{(0)}$ and $\mathbf{C}^{(0)}$ according to the search space. Initialize two evolution paths $\mathbf{p_C}^{(0)} = \mathbf{p}_\sigma{}^{(0)} = \mathbf{0}$.
2. **while** a termination condition is not satisfied **do**
3. Step 1
   Generate λ independent samples $\left(\mathbf{z}_i\right)_{i=1,\cdots,\lambda}$ from the normal distribution $N(\mathbf{0}, \mathbf{I})$. Compute solution set $\left(\mathbf{x}_i\right)_{i=1,\cdots,\lambda}$ as $\mathbf{y}_i = \mathbf{B}\mathbf{z}_i$ and $\mathbf{x}_i = \mathbf{m}^{(t)} + \sigma^{(t)}\mathbf{y}_i$, where $\mathbf{B}$ is an arbitrary real matrix satisfying $\mathbf{C}^{(t)} = \mathbf{B}\mathbf{B}^T$.
4. Step 2
   Compute objective functions $\mathbf{f}\left(\mathbf{x}_i\right)$ and sort them in ascending order as $\left(\mathbf{x}_{i:\lambda}\right)_{i=1,\cdots,\lambda}$. Here, $\mathbf{x}_{i:\lambda}$ indicates the i-th best solution among λ candidates. Hereafter, $\mathbf{y}_i$ and $\mathbf{z}_i$ corresponding to $\mathbf{x}_{i:\lambda}$ are represented as $\mathbf{y}_{i:\lambda}$ and $\mathbf{z}_{i:\lambda}$.
5. Step 3
   Compute the weighted average of $\left(\mathbf{y}_{i:\lambda}\right)_{i=1,\ldots,\lambda}$ as $\mathbf{dy} = \sum_{i=1}^{\lambda} w_i\,\mathbf{y}_{i:\lambda}$. Then, update the evolution paths as follows:
   $\mathbf{p}_\sigma{}^{(t+1)} = \left(1-c_\sigma\right)\mathbf{p}_\sigma{}^{(t)} + \left(c_\sigma\left(2-c_\sigma\right)\mu_w\right)^{1/2}\sqrt{\mathbf{C}^{(t)}}^{-1}\mathbf{dy}$
   $\mathbf{p_C}^{(0)} = \left(1-c_\sigma\right)\mathbf{p_C}^{(t)} + \left(c_c\left(2-c_\sigma\right)\mu_w\right)^{1/2}\mathbf{dy}$
   Here, μ_w is defined as $\mu_w = 1/\sum_{i=1}^{\lambda} w_i^2$, c_σ and c_c are the cumulation factors for evolution paths, and $\sqrt{\mathbf{C}^{(t)}}$ is the unique and symmetric matrix satisfying $\mathbf{C}^{(t)} = \left(\sqrt{\mathbf{C}^{(t)}}\right)^2$.

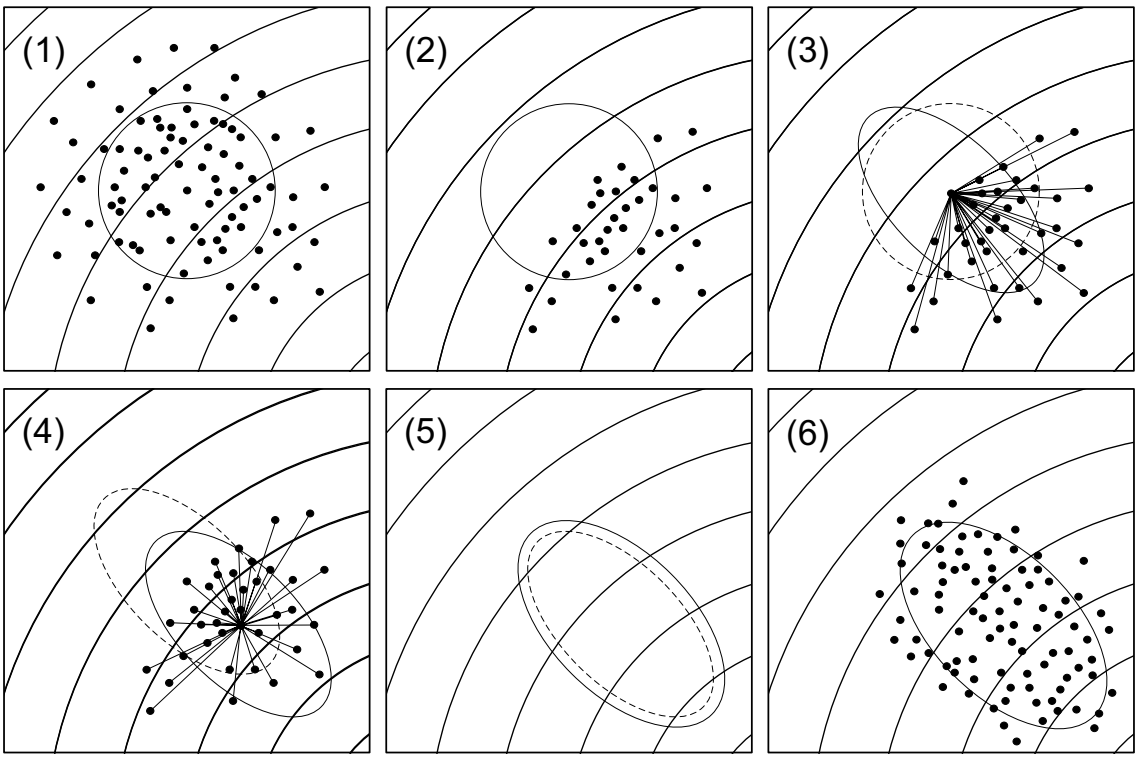

Fig. 2 Schematic of the CMA-ES procedure: (1) Generate multiple candidate solutions. (2) Evaluate and rank the solutions based on the objective function. (3) Update the covariance matrix. (4) Shift the center of the distribution to the weighted mean vector. (5) Update step size. (6) Generate multiple candidates at the next step

Algorithm: CMA-ES

6. Step 4
Update the parameters:
$\mathbf{m}^{(t+1)} = \mathbf{m}^{(t)} + c_m \sigma^{(t)} \mathbf{dy}$
$\sigma^{(t+1)} = \sigma^{(t)} \exp\left[\frac{c_\sigma}{d_\sigma}\left(\frac{\left\|\mathbf{p}_\sigma^{(t+1)}\right\|}{\chi_d} - 1\right)\right]$
$\mathbf{C}^{(t+1)} = \mathbf{C}^{(t)} + c_1\left[\mathrm{OP}\left(\mathbf{p}_c^{(t+1)}\right) - \mathbf{C}^{(t)}\right]$
$+c_\mu \sum_{i=1}^{\lambda} w_i\left[\mathrm{OP}\left(y_{i:\lambda}\right) - \mathbf{C}^{(t)}\right]$
Here, $\mathrm{OP}(\mathbf{v}) = \mathbf{v}\,\mathbf{v}^T$ is the tensor product and χ_d is the expected value$E[\|N(\mathbf{0}, \mathbf{I})\|]$ of the norm of the d-dimensional normal distribution, whose approximated value $d^{1/2}\left(1 - \frac{1}{4d} + \frac{1}{21d^2}\right)$ is used. The coefficients c_m, c_1 and c_μ are the learning rates for the mean vector update, the rank-one covariance update and the rank-μ covariance update, respectively. The damping factor for σ-update is denoted by d_σ.
7. **end while**

All the strategy parameters such as learning rates are set to their default values [33]. Since we apply a restart strategy, termination conditions for each run must be carefully chosen. We apply two termination conditions. Two stopping conditions are used for restarts. We restart the CMA-ES with the double population size if the coordinate-wise standard deviations of the sampling distribution are all smaller than 10^{-12} (small distribution), or if the inter-quartile ranges of the function values in the last $20 + 3d/\lambda$ iterations are smaller than the trace of the covariance matrix of the sampling distribution times $10^{-12} \cdot d$ (low function value variation). The optimization itself is stopped after $10^6 \cdot d$ function evaluations.

5 Numerical Results

As stated before, the subject ship was MV Esso Osaka, and the calculations were carried out in model scale. In the beginning, the authors showed the behavior in a stop maneuver. Figure 3 indicates the trajectory with a certain initial forward speed in the stop maneuver. As can be seen, in the stopping process, the ship's bow makes a turn to starboard because of single propeller. Therefore, it is believed that these characteristics should be positively utilized in the

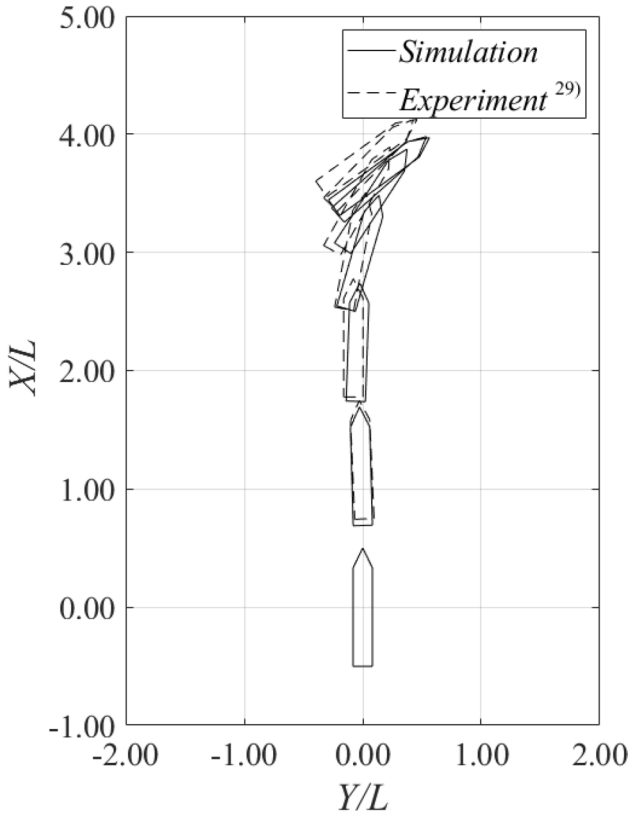

Fig. 3 Emergency stop maneuver

berthing calculations. Otherwise, the final condition and constraints would not be rigorously satisfied.

First, the calculation results with an initial heading angle of 0° and final heading angle of 0° at berth are shown in Fig. 4. In this paper, this calculation condition is called case 1. In the upper-left figure, the dashed line indicates the final Y position, and this line is parallel to the berth with a distance of $0.9B$. As stated above, in its computation, preparation of the prior solution is not necessary at all, and the optimal solution is stochastically searched using a multidimensional normal distribution. From this figure, since the final state variables have converged to zero, it is understood that a two-point boundary value problem is successfully solved. From the obtained trajectory, it is observed that collision does not occur. The rudder input in this maneuver slightly shows the behavior of bang–bang control, in which the control variable switches the maximum and minimum values. However, for the propeller revolution number, this tendency is not clearly observed. However, the switching of positive and negative values is frequently observed. Although a typical vessel with a diesel engine cannot establish frequent switching, an electric propulsion vessel or one equipped with a CPP has the capability of achieving this control.

The convergence process in the optimization is shown in Fig. 5. The upper-left and upper-right figures show the transition of the best objective function value obtained at each iteration (in linear scale) and the difference of the objective function value from the minimum function value obtained during the single run (in logarithmic scale). The lower-left and lower-right figures show the transition of the square root of the eigenvalue of the covariance matrix and the square root of the diagonal element of the covariance matrix, respectively. Note that the square root of each eigenvalue represents the length of each axis of the equi-density ellipsoid, whereas the square root of each diagonal element represents the standard deviation in each coordinate. Difference in these two figures indicates that the equi-density ellipsoid is not aligned in the given coordinate, and the CMA-ES learns variable dependencies. There appear several spikes, and they indicate the restarting strategy of the CMA-ES. From this figure, at each restart, the finally converged objective function is different. At each restarting, the population size is increased by a factor of 2, and the introduction of restarting contributes to the capability of the global search. In this result, after the first restarting, the best objective function was obtained.

Since the CMA-ES based upon the stochastic search, the final results depend on the stochastic seeds. Table 4 shows the statistics of the results of 10 independent trials of the CMA-ES. First of all, it is noteworthy that the collision to the berth was perfectly avoided. In the proposed method, the terminal constraint is included in performance index as penalty using weight. Therefore, t_f and $w_1|\mathbf{x}(1)-\mathbf{x}_0|$ have a trade-off relation. In all of the trials, the proposed method using the CMA-ES successfully provided the feasible maneuver without giving the good initial guess. In this sense, it is considered that the proposed method is a robust method.

Next, the calculation results with an initial heading angle of 180° and final heading angle of 180° at berth are shown in Fig. 6. In this paper, this calculation condition is called case 2. In this figure, it should also be noted that the two-point boundary value problem is successfully solved with the CMA-ES. The obtained optimal rudder input clearly shows a bang–bang-type input.

As we mentioned, in the astern condition with forward velocity, the subject ship "ESSO OSAKA" has a tendency that the heading angle becomes positive. Therefore, as can be seen in Fig. 4 (case 1), when reducing heading speed, heading angle tends to port side. As a result, ship tends meandering. On the other hand, in this case (case 2), although she uses the negative speed, the maneuver is considered to be easier than case 1 because of the tendency shown in Fig. 3.

The convergence process in the optimization is shown in Fig. 7. In this result, after the second restarting, the best

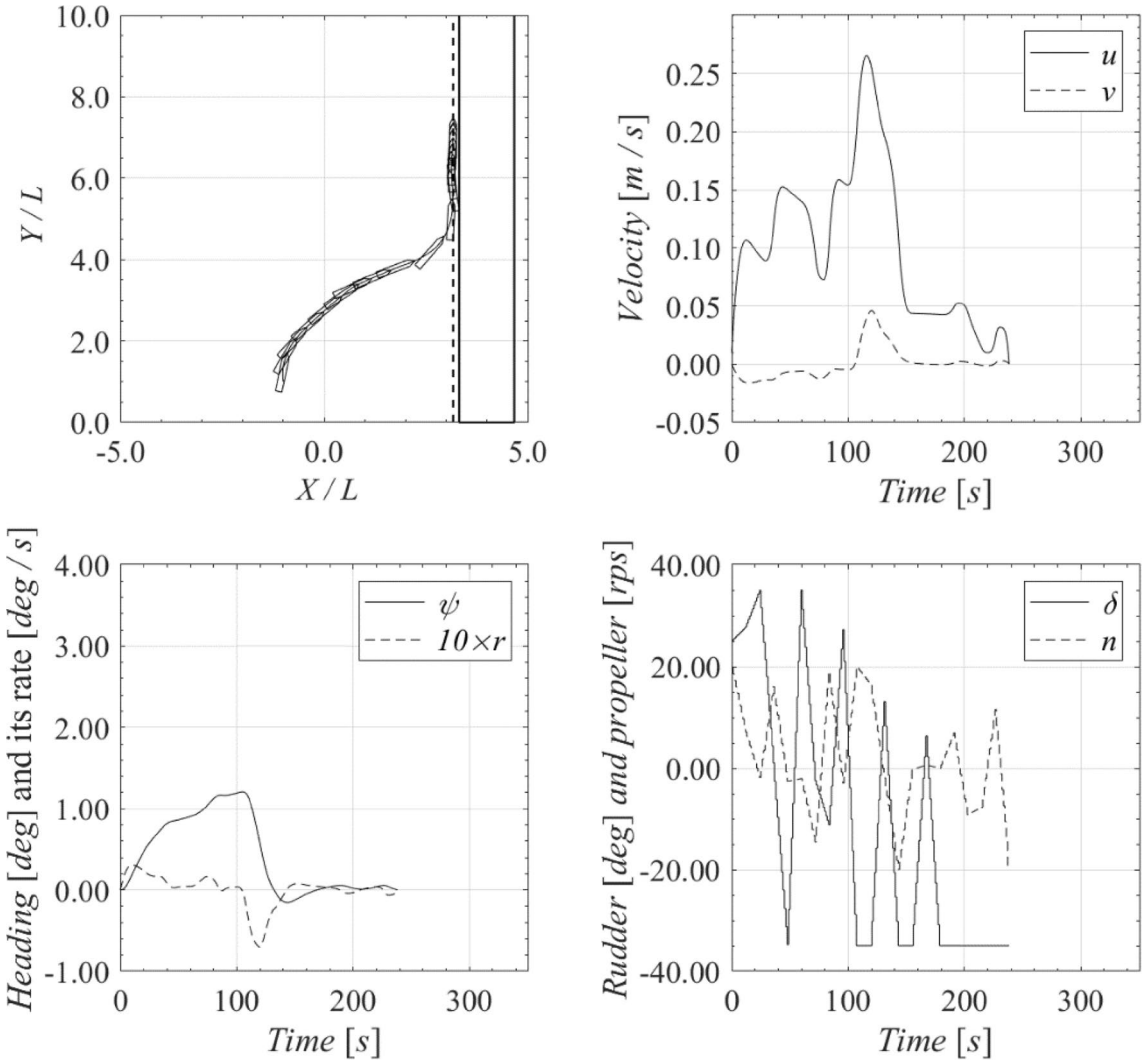

Fig. 4 Berthing maneuver (case 1)

objective function is obtained; whereas after a third restarting, an inferior result is obtained. This tendency means that the problem dealt with here has many local optima, and the gradient-based method could fail to search.

If we carefully examine the present results, it is understood that the final state values do not completely match the given condition. For instance, in right-upper panel in Fig. 4, r has non-zero value in the final state. To satisfy the final condition rigorously, the weight w_1 should be increased. However, using a larger w_1 reduces the capability to reduce the final time in this formulation. Therefore, the algorithm in which the inequality constraints are taken into account must be applied in our future research.

As stated above, in this example as well, there appeared several positive–negative switches of the propeller revolution number. Although a typical diesel engine cannot achieve such rapid switching, an electric propulsion vessel can do it. However, for practical purposes, constraints should be imposed on the number of switches in future works. Further, constraints on rudder speed limitation should be imposed as well.

Since the proposed algorithm is offline, the computation time is not a concern. Typically, it could take a couple of hours. Therefore, we cannot directly apply this method to an online calculation. On the other hand, the obtained results can be applied for the initial solution of the online calculation method such as C/GMRES. Furthermore, in this research, the errors between the mathematical model and the actual system, such as model error, scale effect, wind disturbance and so on, are not taken into account. To absorb these errors, the application of the online algorithms is considered to be useful. Its application is one of our planned future works.

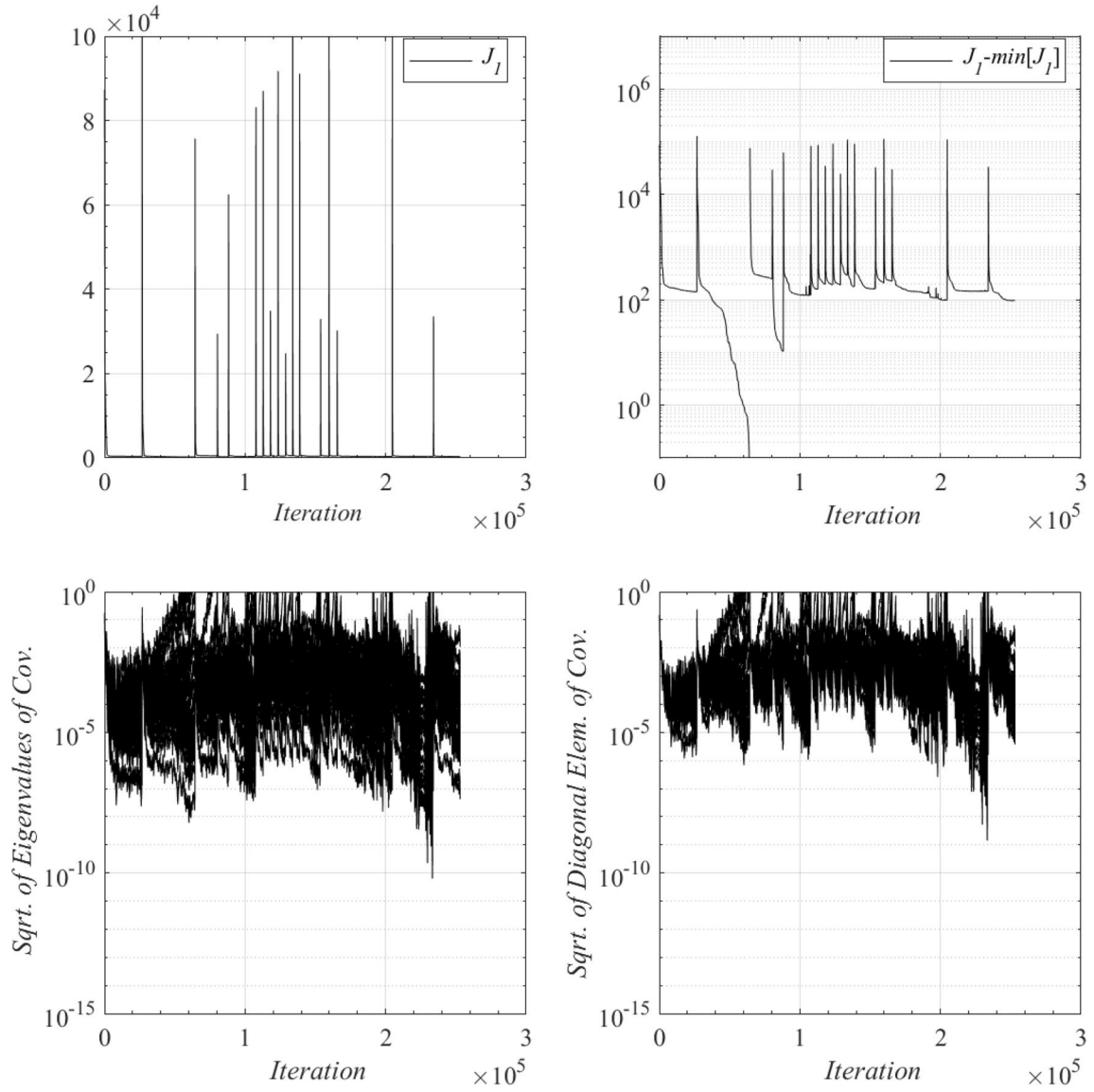

Fig. 5 Optimization process (case 1). Displayed are $J_1(\mathbf{X})$ in linear (upper left) and log scale of $J_1(\mathbf{X})$–min$[J_1(\mathbf{X})]$ (upper right), square root of the eigenvalues of the covariance matrix (lower left) and square root of the diagonal elements of the covariance matrix (lower right)

Table 4 Statistical analysis results in 10 results

	Min	Max	First quartile	Second quartile	Third quartile	Average	Standard deviation
t_f	1.684E+02	2.675E+02	1.998E+02	2.237E+02	2.427E+02	2.186E+02	3.341E+01
$w_1\lvert\mathbf{x}(1)-\mathbf{x}_0\rvert$	2.838E+00	9.721E+01	7.794E+00	2.045E+01	5.095E+01	3.137E+01	3.081E+01
w_2C	0.000E+00	0.000E+00	0.000E+00	0.000E+00	0.000E+00	0.000E+00	0.000E+00

6 Concluding remarks

In this research, the optimal berthing problem was modeled as a minimum-time problem, in which the collision risk was taken into account. Although the problem to be solved was highly nonlinear, its difficulty was successfully overcome by introducing the CMA-ES as a solver of the optimization. Then, the optimal solution that satisfied every condition was finally calculated without preparing high-quality, feasible prior solutions; therefore, the proposed method was

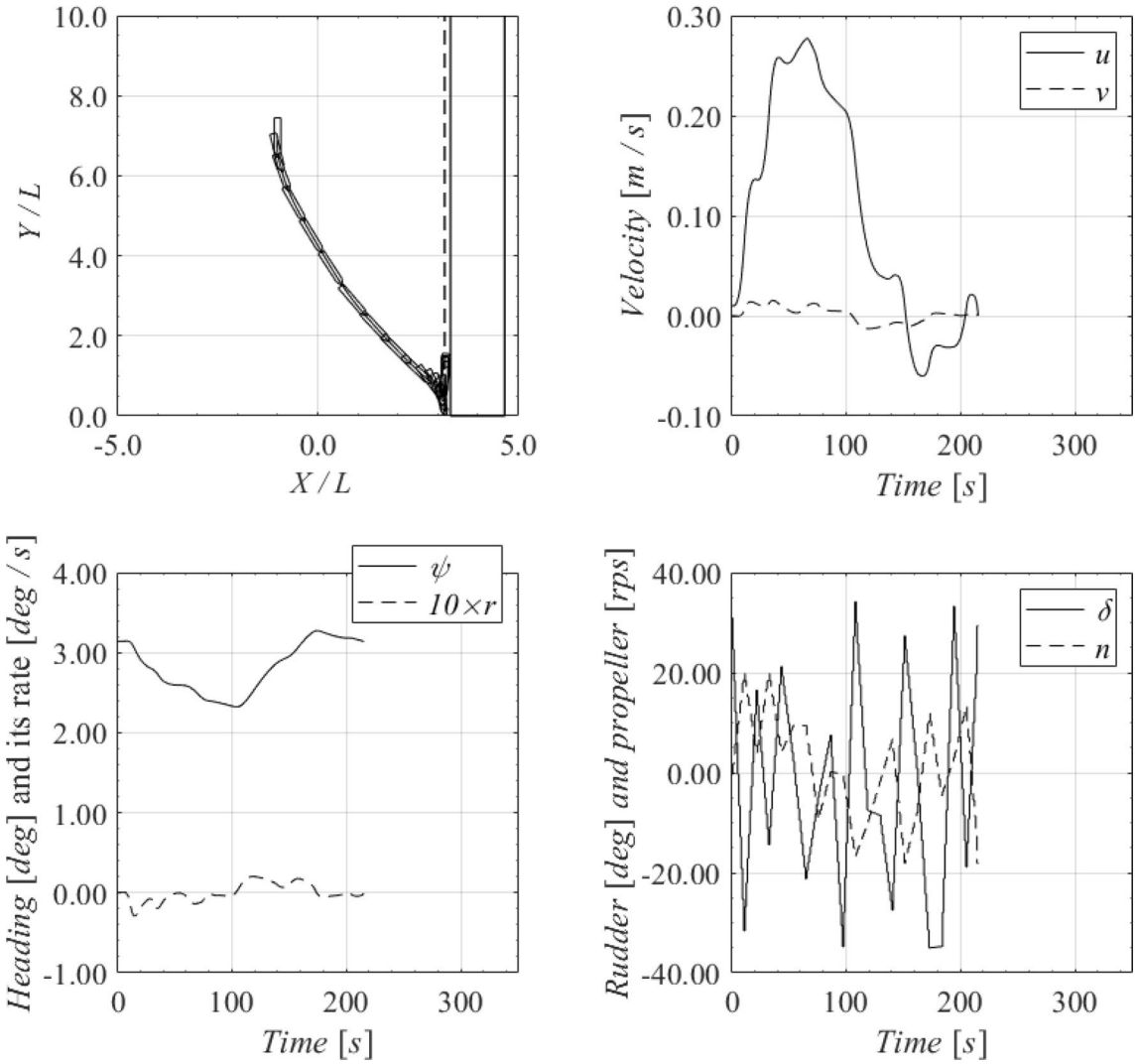

Fig. 6 Berthing maneuver (case 2)

robust. In the obtained results, there appeared several positive–negative switches in the propeller revolution number. Although a typical diesel engine cannot achieve such rapid switching, an electric propulsion vessel can do it. However, for practical purposes, an algorithm in which constraints are imposed on the number of switches is essential. Simultaneously, concerning with rudder activity, the constraints on the rudder speed should be taken into account. This will be one of our future tasks. Furthermore, adjustment of included two weights in the performance index should be avoided by introducing Lagrangian constraint handling method [32]. This will be one of our future tasks. In this research, vessels having only a rudder and propeller were considered, but as a next step, the optimal control of vessels with bow/stern thrusters, CPPs, and high-performance rudders such as the Vec-Twin rudder system should be investigated. Furthermore, although the obtained results were offline, the online methods could be applied for the initial solution of online control such as C/GMRES. This is also one of our future tasks.

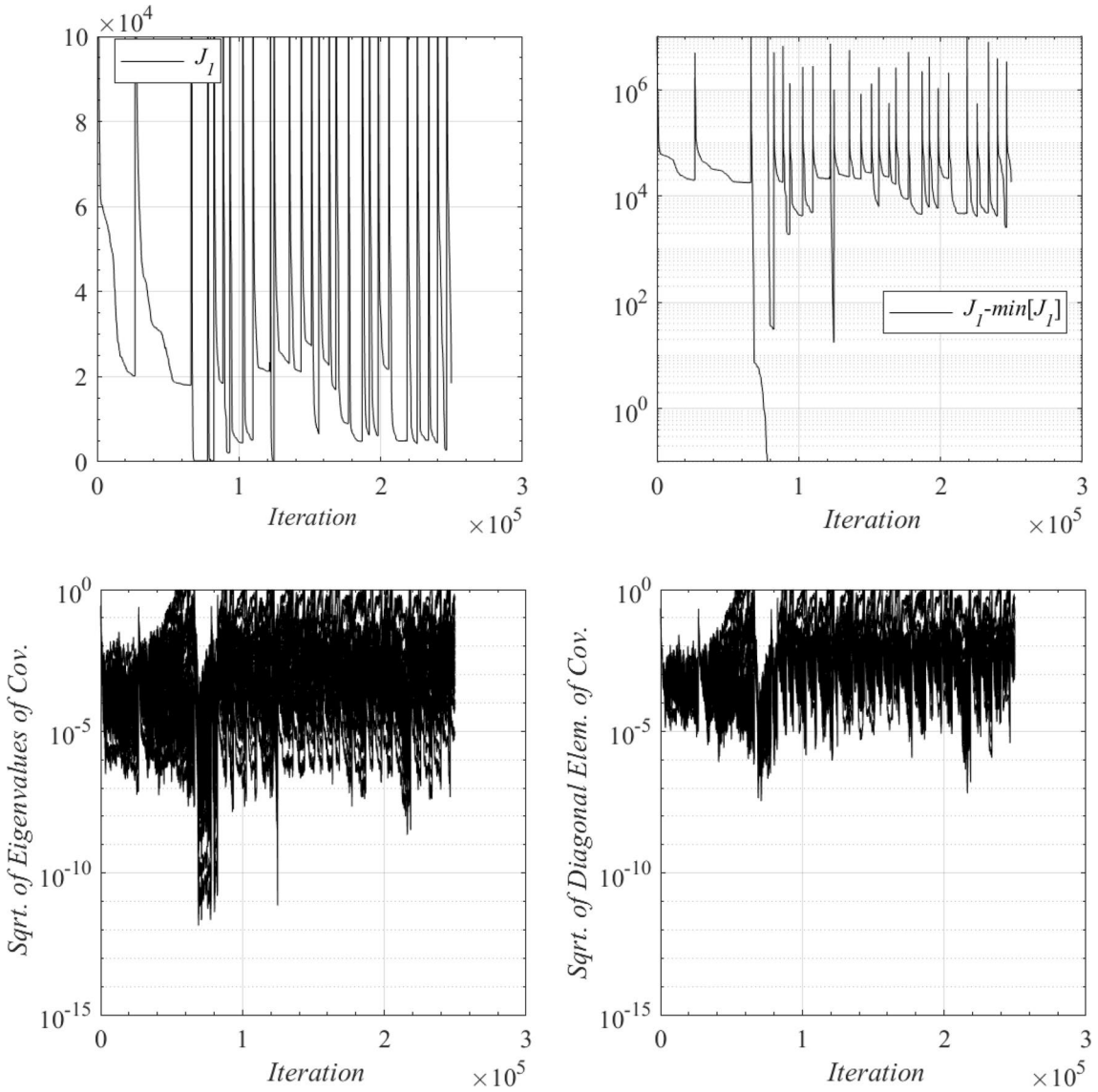

Fig. 7 Optimization process (case 2). Displayed are $J_1(\mathbf{X})$ in linear (upper left) and log scale of $J_1(\mathbf{X})$–min$[J_1(\mathbf{X})]$ (upper right), square root of the eigenvalues of the covariance matrix (lower left) and square root of the diagonal elements of the covariance matrix (lower right)

Acknowledgements The authors are grateful to Mr. Koichi Shouji and Dr. Satoshi Masuda in JMU (Japan Marine United Corporation) for their technical advices and discussions. This work was supported by FY2018 Fundamental Research Developing Association for Shipbuilding and Offshore (REDAS) in Japan. The authors would like to thank Enago (http://www.enago.jp) for the English language review.

References

1. http://www.unmanned-ship.org/munin/. Accessed 25 June 2018
2. http://www.rolls-royce.com/~/media/Files/R/Rolls-Royce/documents/customers/marine/ship-intel/rr-ship-intel-aawa-8pg.pdf. Accessed 25 June 2018
3. Takai T, Yoshihisa H (1987) An automatic maneuvering system in berthing. In: Proceedings, 18th ship control symposium, vol 2. The Hague
4. Takai T, Ohtsu K (1990) Automatic berthing experiments using "Shioji-Maru" (in Japanese). J Jpn Inst Navig 83:267–276
5. Hasegawa K (1998) Measurement and control techniques of ships. Measurement and control for safety navigation (in Japanese). J Soc Instrum Control Eng 37(11):762–767
6. Kose K, Fukudo J, Sugano K, Akagi S, Harada M (1986) On a computer aided maneuvering system in harbors (in Japanese). J Soc Nav Arch Jpn 160:103–110
7. Koyama T, Jin Y, Jin KH (1987) A systematic study on automatic berthing control (1st report) (in Japanese). J Soc Nav Arch Jpn 162:201–210
8. Yamato H, Uetsuki T, Koyama T (1990) Automatic berthing by the neural controller. In: Proceedings of 9th ship control systems symposium, vol 3, pp 183–201

9. Hasegawa K, Kitera K (1993) Automatic berthing control system using network and knowledge-base (in Japanese). J Kansai Soc Nav Arch 220:135–143
10. Yamato H, Koyama T, Nakagawa T (1993) Automatic berthing system using expert system (in Japanese). J Soc Nav Arch Jpn 174:327–337
11. Shouji K, Ohtsu K (1992) A study on the optimization of ship maneuvering by optimal control theory (1st report) (in Japanese). J Soc Nav Arch Jpn 172:365–373
12. Wu AK, Miel A et al (1980) Sequential conjugate gradient–restoration algorithm for optimal control problems with nondifferential constraints and boundary conditions Part l. Optim Control Appl Methods 1:69–88
13. Shouji K, Ohtsu K, Hotta T (1993) A study on the optimization of ship maneuvering by optimal control theory (2nd report) (in Japanese). J Soc Nav Arch Jpn 173:221–229
14. Shouji K, Ohtsu K (1993) A study on the optimization of ship maneuvering by optimal control theory (3rd report) (in Japanese). J Soc Nav Arch Jpn 174:339–344
15. Okazaki T, Ohtsu K, Shouji K, Mizuno N (1996) A study on the minimum time stopping problem (in Japanese). J Soc Nav Arch Jpn 180:223–234
16. Ohtsuka T (2004) A continuation/GMRES method for fast computation of nonlinear receding horizon control. Automatica 40(4):563–574
17. Hamamatsu M, Kagaya H, Kohno Y (2008) Application of nonlinear receding horizon control for ship maneuvering (in Japanese). Trans Soc Instrum Control Eng 44(8):685–691
18. Mizuno N, Uchida Y, Okazaki T (2015) Quasi real-time optimal control scheme for automatic berthing. In: 10th IFAC conference on maneuvering and control of marine craft MCMC 2015, vol 48, issue 16, pp 305–312
19. Maki A, Umeda N, Ueno S (2008) Application of optimal control theory to course keeping problem in following seas (in Japanese). J Jpn Soc Nav Arch Ocean Eng 7:207–212
20. Maki A, Umeda N, Ueno S (2008) Investigation on broaching-to using optimal control theory. J Jpn Soc Nav Arch Ocean Eng (in Japanese) 8:115–122
21. Hansen N (2006) The CMA evolution strategy: a comparing review. In: Lozano JA, Larrañaga P, Inza I, Bengoetxea E (eds) Towards a new evolutionary computation. Springer, Berlin, Heidelberg, pp 75–102
22. Hansen N, Auger A (2014) Principled design of continuous stochastic search: from theory to practice. In: Borenstein Y, Moraglio A (eds) Theory and principled methods for designing metaheustics. Springer, Berlin, Heidelberg, pp 145–180
23. Yokoyama N, Suzuki S (2003) A numerical method for optimal control problem using genetic algorithm (in Japanese). J Jpn Soc Aeronaut Space Sci 51(592):207–214
24. Kita H, Ono I, Kobayashi S (2000) Multi-parental extension of the unimodal normal distribution crossover for real-coded genetic algorithms (in Japanese). Trans Soc Instrum Control Eng 36:875–883
25. Yasukawa H, Yoshimura Y (2015) Introduction of MMG standard method for ship maneuvering predictions. J Mar Sci Technol 20:37–52
26. Yoshimura Y, Nakao I, Ishibashi A (2008) Unified mathematical model for ocean and harbor maneuvering. In: Proceedings of the international conference on marine simulation and ship maneuverability 2009, pp 116–124
27. ITTC (2002) Final Report and Recommendations to the 23rd ITTC: the specialist committee on Esso Osaka. In: The proceedings of the 23rd ITTC conference
28. Ueda N (1985) On the maneuvering motion of a vessel during backing (in Japanese). Master thesis, Osaka University
29. Hachii T (2004) The prediction of maneuvering motion on ships with low speed using standard MMG model (in Japanese). Master thesis, Osaka University
30. Fujii H, Tuda T (1961) Experimental research on rudder performance (2) (in Japanese). J Soc Nav Arch Jpn 110:31–42
31. Kose K, Hinata H, Hashizume Y, Futagawa E (1984) On a mathematical model of maneuvering motions of ships in low speeds (in Japanese). J Soc Nav Arch Jpn 155:132–138
32. Atamna A, Auger A, Hansen N (2016) Augmented lagrangian constraint handling for CMA-ES—case of a single linear constraint. In: Proc. of the parallel problem solving from nature—PPSN II, Cham, vol 9921, no 2, 2nd edn, pp 181–191
33. Hansen N (2016) The CMA evolution strategy: a tutorial. arXiv :1604.00772
34. Sakamoto N, Akimoto Y (2017) Improvement to the box constraint handling method for the CMA-ES and its generalization to linear constraints (in Japanese). Trans Jpn Soc Evolut Comput 8(2):23–35
35. Sakamoto N, Akimoto Y (2017) Modified box constraint handling for the covariance matrix adaptation evolution strategy. In: Genetic and evolutionary computation conference, Berlin, Germany, July 15–19, 2017, companion material proceedings, pp 183–184
36. Auger A, Hansen N (2005) A restart CMA evolution strategy with increasing population size. In: Proc. of the 2005 IEEE congress on evolutionary computation, pp 1769–76
37. Akimoto Y, Nagata Y, Ono I, Kobayashi S (2012) Theoretical foundation for CMA-ES from information geometry perspective. Algorithmica 64(4):698–716